



HAL
open science

Transient oxidation of hazes a source of nutrients during the great oxidation event

Louis Maratrat, Yassin Jaziri, Maëva Millan, Valentin Moulay, Ludovic Vettier,
Théo Govekar, Alex Abello, Nathalie Carrasco

► **To cite this version:**

Louis Maratrat, Yassin Jaziri, Maëva Millan, Valentin Moulay, Ludovic Vettier, et al.. Transient oxidation of hazes a source of nutrients during the great oxidation event. *Scientific Reports*, 2025, 15 (29284), pp.29284. <10.1038/s41598-025-13441-1>. <hal-05217709v2>

HAL Id: hal-05217709

<https://hal.science/hal-05217709v2>

Submitted on 2 Sep 2025

HAL is a multi-disciplinary open access archive for the deposit and dissemination of scientific research documents, whether they are published or not. The documents may come from teaching and research institutions in France or abroad, or from public or private research centers.

L'archive ouverte pluridisciplinaire **HAL**, est destinée au dépôt et à la diffusion de documents scientifiques de niveau recherche, publiés ou non, émanant des établissements d'enseignement et de recherche français ou étrangers, des laboratoires publics ou privés.



HAL Authorization



OPEN Transient oxidation of hazes a source of nutrients during the great oxidation event

L. Maratrat¹✉, A. Y. Jaziri¹, M. Millan¹, V. Moulay¹, L. Vettier¹, T. Govekar¹, A. Abello¹ & N. Carrasco^{1,2}

The transition period of the Great Oxidation Event (GOE) saw the emergence of transient physical and chemical processes. In this context, photochemical organic hazes may have evolved in an atmosphere containing low concentrations of oxygen ($<10^{-5}/10^{-6}$ Present Atmospheric Level). This coexistence of organic aerosols and oxygen traces induced an atmospheric reactivity which has so far been unexplored. Here, we show that the progressive rise of oxygen around the GOE triggered oxidation of organic aerosols suspected to be present at that time. We estimate that such transient mechanisms would have persisted over 60 to 100 Myrs during the GOE and possibly extended during the Archean. The main chemical markers of aerosol oxidation observed are urea, oxalic acid and carboxylic acid derivatives. These oxygen-bearing organics identified could have served as nutrients by existing ecosystems. This input of oxidized organic matter, estimated between 10^{13} and 10^{15} g of C.yr⁻¹ based on aerosol production yields, has probably been significant compared to oxygenic photosynthesis. Such mechanisms could also have diversified the pool of available nutrients, constituting an interesting vector of biodiversity for the primitive ecosystem.

The Great Oxidation Event (GOE) is a major period estimated to have happened between 2.4 and 2.1 billion years ago and marked deep changes in the atmosphere of the Early-Earth. It went from a reduced atmosphere at the end of the Archean era to the significantly oxidized Proterozoic environment. In the Archean era, the atmospheric composition of the Early-Earth was notably reduced with very low O₂ atmospheric level in comparison to present days. One of the best constraint on O₂ proportion is given by S-MIF (Sulfur-Mass Independent Fractionation) observed in sulfide and sulfate minerals of Precambrian rocks^{1,2}. Such isotopic anomalies are considered to result from SO₂ photochemistry³ which is only active under a sufficiently reduced atmosphere⁴. Indeed, energetic UV light penetrates and dissociates SO₂ only in a reduced atmosphere deprived of the ozone layer. An upper limit for oxygen is estimated in the Archean atmosphere between 10^{-6} and 10^{-5} PAL (Present Atmospheric Level) (0.2 ppm to 2 ppm)^{5,6}. In this anoxic Archean world, the atmosphere is thought to be mainly dominated by N₂ as well as significant amounts of CO₂^{7,8} and CH₄^{6,8-10} with no precise constraints on their respective abundancies. However, CH₄ produced by methanogenesis was certainly more abundant in the early atmosphere than today^{11,12} in absence of photochemical oxidative sinks. More precisely, photochemical models estimate an order of magnitude of 1000 ppm for CH₄ supposing an actual efficient microbial surface flux in the Archean era^{13,14}.

This atmospheric composition with a significant amount of methane could have been favorable to the formation of organic hazes, considering the chemistry occurring in the atmosphere of Titan, the largest moon of Saturn¹⁵. Such hazes may have had a major influence on the global climate of the Early-Earth due to their radiative properties potentially leading to a global cooling or “anti-greenhouse” effect^{16,17} as well as a UV protection affecting NH₃ photochemistry¹⁸. However, the existence of organic hazes is still an open question. S-MIF attenuation during the Mesoarchean^{2,19-21} and C¹³ depletion in sediments^{11,12,22} support episodic haze formations. With a very different approach, laboratory experiments reproducing the Archean photochemistry^{23,24} also argue in favor of the existence of organic hazes during this era. Then, the GOE (2.4–2.1 Ga) has been detrimental to anoxygenic methanogens triggering a decrease in methane surface emission, thus progressively leading to the disappearance of organic hazes.

During this transition, transient geo-chemical processes influenced the Early-Earth system on a global scale, playing an important role in its evolution. Our work focuses on the peculiar evolution of photochemical hazes. In this transition regime, notably in the beginning of the GOE, organic hazes coexisted with traces of oxidizing species due to the rise of oxygen produced by photosynthetic life. These interactions with trace

¹Université Paris-Saclay, UVSQ, CNRS, LATMOS, Guyancourt 78280, France. ²ENS-Paris-Saclay, Gif sur Yvette 91190, France. ✉email: louis.maratrat@latmos.ipl.fr

atmospheric oxidizers induced chemical transformations on the aerosols which has never been addressed so far. More precisely, the atmosphere could have offered favorable conditions for the occurrence of haze heterogenous oxidation processes. The concomitant presence of photochemical aerosols produced efficiently by methane photochemistry on the one side and a more important concentration of oxidized species at the surface on the other side could have triggered efficient oxidation ageing processes as those observed in the present Earth atmosphere²⁵. Yet, such atmospheric heterogenous mechanisms constitute an interesting source of oxygen and nitrogen-bearing organic molecules²⁶ before any interaction with liquid water, providing a global input of evolved organic matter at the surface potentially utilizable by the biosphere.

To investigate experimentally these interactions and their implications in the context of the Archean and the GOE, we considered a starting pool of reduced haze analogues containing nitrogen (haze particles made of only $C_xH_yN_z$ molecules) as a model case of reducing matter for Early-Earth hazes. We exposed this material to a weakly oxidative N_2 atmosphere plausible for the Archean (and the beginning of the GOE) in term of oxidation level (1 ppm of H_2O and 0.1 ppm of O_2) to study its evolution in such atmospheric conditions. Then, we searched for the presence of oxygen-bearing molecules, which, in this case, are directly indicative of an oxidation process. The analytical characterization of these organic molecules has been performed using gas chromatography coupled with mass spectrometry (GC-MS).

Results

Identification of oxygen-bearing molecules: a tracer of aerosol reactivity in weakly oxidative conditions

Eight oxygen-bearing compounds are revealed in our samples by analyzing the GC-MS data.

The measurements were repeated in triplicates and blanks were performed to confirm that the molecules of interest were distinct from any contamination sources that may have occurred during the storage and the sample preparation protocol prior to the injection into the GC. The sub-figures presented in Fig. 1 show the comparative chromatograms between the blank and the haze analogs after storage under the chosen experimental conditions (0.1 ppm O_2 , 1 ppm H_2O). The Extracted Ion Chromatograms (EIC) related to each oxygen-bearing compound show a significant increase of their relative intensities compared to the blank. The m/z chosen for these EIC are specified (Fig. 1). For all the molecules, the signal over noise ratio is superior to 3 which is meaningful.

The eight species targeted were identified through their mass spectra (see Figure S-1 in supplementary material) compared to their corresponding reference from the National Institute of Standard and Technology (NIST) spectral database. The identification of the molecules were also confirmed using the retention times of the standard molecules ran within the same GC-MS conditions. To strictly confirm these identifications and the oxidation process involved, we voluntarily exposed the sample to the ambient atmosphere. This increased the efficiency of the oxidation processes and thus subsequently increased the abundance of the oxygenated molecules produced. In such conditions, the mass spectra obtained for the oxidized sample matched the NIST standard (see supplementary materials, Figure S-2).

Figure 1 revealed the formation of eight oxygenation products: carbamic acid, dimethylcarbamic acid, oxalic acid, glycine, urea, hydroxylamine, ammeline and 5-azacytosine. Such chemical structures are represented in Fig. 2. The products observed mainly result from the reactivity of OH radicals on the organic haze matrix. OH radicals are known to react on unsaturation to produce keton derivatives²⁷ as urea. Moreover, OH radicals also add on aromatic hydrocarbons leading to the formation of hydroxy aromatics²⁸ like ammeline and 5-Azacytosine. These remarks highlight the common points existing between the reactivity of the organic haze matrix studied and the one of reduced Volatile Organic Compounds in the Earth troposphere mainly controlled by OH radicals²⁵.

Figure 2 shows the wide diversity of the oxygen-bearing organic functions formed through oxidation of the reduced haze analogue with the presence of carboxylic acids, ketone, and alcohols. These findings are consistent with previous works that studied the properties and the reactivity of reduced haze analogues after hydrolysis in acidic or basic conditions, and have shown the formation of amino acids, diacids and urea^{29–31}. Results presented in this study show that atmospheric dry mechanisms lead to the same species, without the assistance of liquid water. In addition, we show that 1,3,5-triazines are the only oxygen and nitrogen-bearing aromatic species identified here. Their formation could be favored by the high abundance of Triazine in the aerosol analogues as suggested by several studies^{32–35}.

These results and the formation of oxygen species confirm the possibility for reduced organic compounds contained within an aerosol matrix to react with traces atmospheric oxidant species up to the ppm level. The quantity of oxidized products forms has not been specifically quantified here. On exposure times longer than the ten days performed in this study more important yields could be reached. After several months, which represent the typical degradation timescale of haze organics in presence of humidity³⁶ oxidized molecules, and more particularly urea which is the most abundant one, are present in significative proportions in the bulk material. A previous study notably estimated an order of magnitude of 1 mg/g for the mass fraction of urea in similar organic hazes after exposure to ambient air³⁷.

Our results and the previous remarks thus provide experimental evidences of the important role played by atmospheric oxidation processes in the Archean and at the beginning of the GOE.

Aerosol oxidation during the GOE: existence and timescales

Here we investigate the existence of aerosol oxidation during the GOE by constraining more precisely in time the interval during which such processes could have persisted. To do so, we define two necessary conditions for aerosol oxidation, which are the existence of organic aerosols and a sufficient proportion of oxygen reactant in the atmosphere.

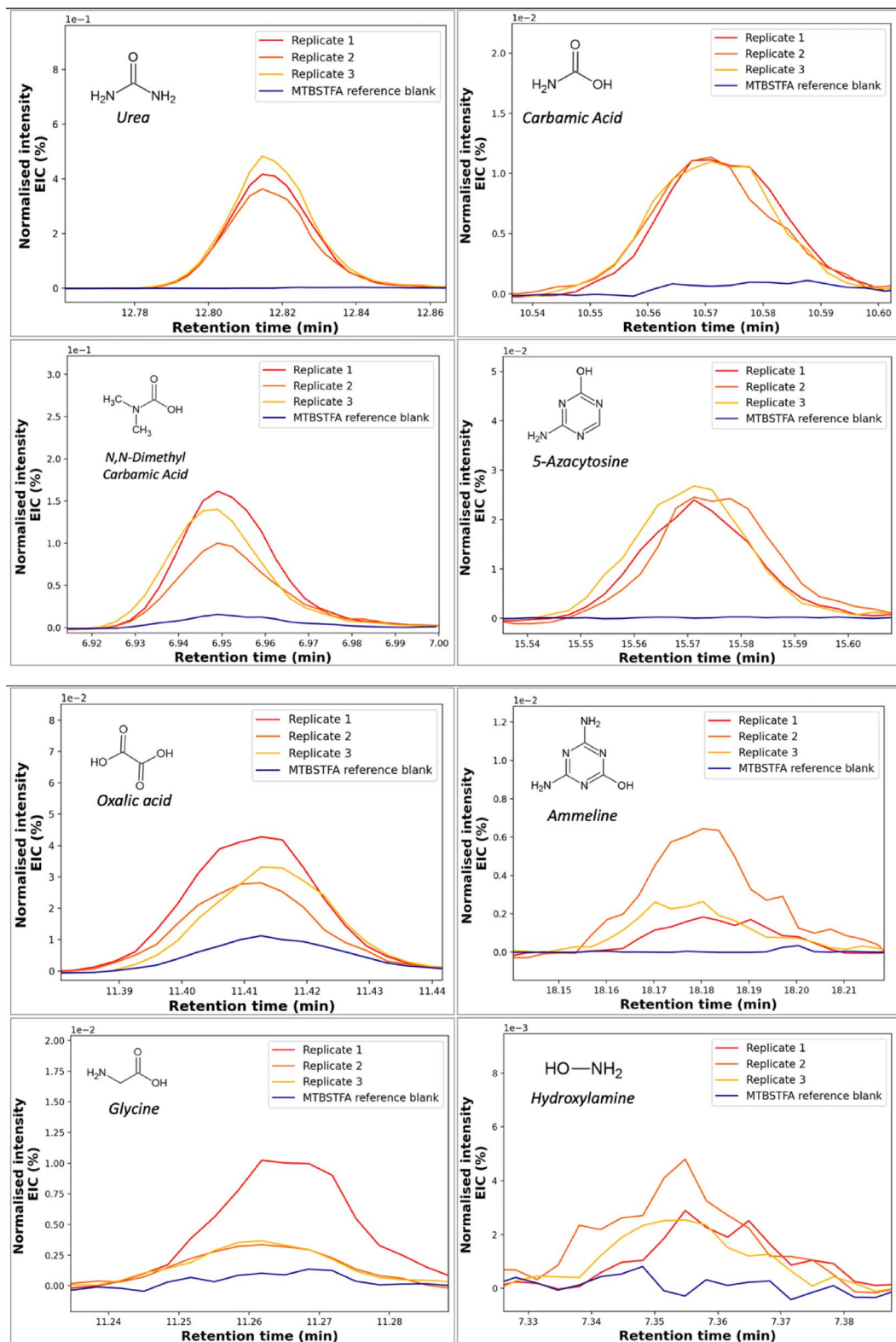


Fig. 1. Extracted Ion Chromatograms (EIC) for the different oxygenated species identified. The fragments used for the sub-figures are respectively: $m/z = 231$ for urea, $m/z = 232$ for carbamic acid, $m/z = 146$ for N, N-Dimethyl carbamic acid, $m/z = 283$ for 5-Azacytosine, $m/z = 261$ for oxalic acid, $m/z = 298$ for ammeline, $m/z = 246$ for glycine, and $m/z = 132$ for hydroxylamine. The signals have been normalized by the maximum intensity of the internal standard peak (Naphtalene-D8) to correct variations in the response of the instrument. For clarity, the signals have also been synchronized (to fix the maximum of the peaks at the same retention time) and their baseline have been corrected.

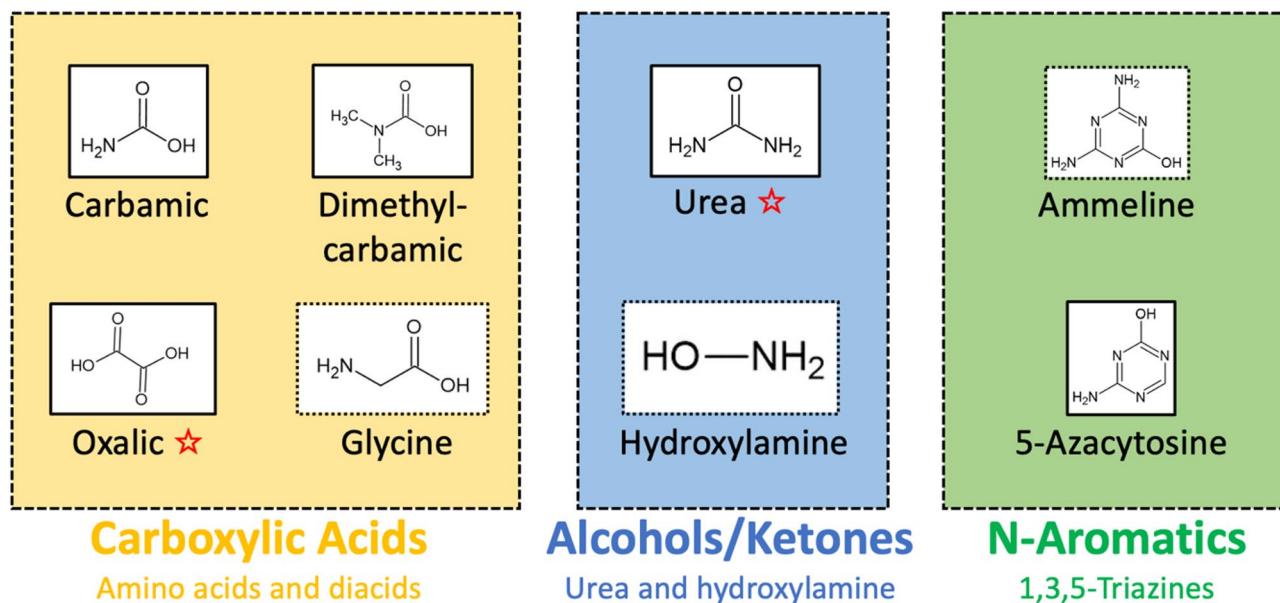


Fig. 2. Chemical structure of the eight oxygen-bearing molecules identified in this study, classified by chemical functions and/or structure similarities. The red star designates the molecules with the most intense signal.

Based on our experimental results, we take an order of magnitude of 0.1 ppm as a limit in O_2 content to trigger oxidation on aerosols.

For organic aerosols, we focus our approach on the variation of atmospheric composition and its associated uncertainty. One key parameter for haze production is the ratio CH_4/CO_2 . Based on a previous experimental study, a criterion for aerosol formation is roughly chosen at $CH_4/CO_2 > 0.1$ ²³. While this criterion works for a majority of mixtures, it can sometimes be restrictive and several counter-examples can be cited: for instance $H_2-CO_2-N_2$ mixtures without CH_4 are also known to produce organic films²⁴. Nevertheless, we used this criterion as an underestimation of the existence of aerosols during the GOE and the Archean.

Figure 3 shows the variations of O_2 volume mixing ratio (vmr) as well as the uncertainties on the ratio CH_4/CO_2 during the Archean and the GOE. O_2 vmr is calculated using the approach described in previous modelling studies³⁸. It takes into account phenomena such as surfaces flux from methanogenesis and photosynthesis, loss by hydrogen escape, and photochemical processes. Moreover, temporal uncertainties on CO_2 and CH_4 have been taken from the following review⁴. Such uncertainties allow to estimate the upper (σ_+) and lower (σ_-) limits for the ratio CH_4/CO_2 thanks to the following relations $\sigma_+(t) = \frac{\max CH_4(t)}{\min CO_2(t)}$ and $\sigma_-(t) = \frac{\min CH_4(t)}{\max CO_2(t)}$.

The envelop on the ratio CH_4/CO_2 shown in Fig. 3, suggests a likely formation of organic aerosols during the Archean and the GOE. The difference between the threshold for aerosol formation $CH_4/CO_2 = 0.1$ (black dashed line) and the upper limit value of this same ratio is quite significant before the GOE. This difference starts decreasing progressively in the GOE but remains in favor of aerosol formation until the 0.1 threshold is crossed. The intersection between the upper envelope of the CH_4/CO_2 ratio and the 0.1 threshold gives a temporal limit for aerosol existence in the GOE (black dot Fig. 3). This critical point is reached at 2.34 Gyrs, so approximately 0.06 Gyrs after the beginning of the GOE (2.4 Gyrs). Such duration is not negligible compared with the 0.3 Gyrs of the GOE in total and represents 20% of this value. Beyond 2.34 Gyrs, the atmosphere is too oxidized and methane depleted to trigger organic aerosol formation.

Furthermore, the temporal variation of O_2 volume mixing ratio (vmr) in Fig. 3 reveals a sufficient level of atmospheric oxidizers to trigger oxidation processes during the existence period of aerosols. The oxygen threshold value of 0.1 ppm $\approx 10^{-7}$ vmr for oxidation is reached around 2.47 Gyrs, and ensures favorable conditions for aerosol oxidation between 2.47 and 2.34 Gyrs. These results suggest that aerosol oxidation processes could have persisted during the GOE over significant timescales of 100 Myrs. Figure 3 also argues for a possible extension of the aerosol oxidation window in the Archean, before the GOE. The Archean “steady-state” value of oxygen is indeed around 10^{-8} vmr ≈ 0.01 ppm and quite close to the oxidation threshold of 0.1 ppm. This concentration is not incompatible with oxidation, notably if we assume longer aerosol exposure times (taking into account their sedimentation and residence times at the surface) than the ten days performed in this work.

To go further, the prediction of O_2 concentrations strongly relies on the net production of O_2 by photosynthesis of the Archean marine ecosystem N (see methods). Figure 3 corresponds to a favorable case for oxidation assuming an already efficient N value, ten times inferior to the net productivity of the modern marine ecosystem ζ . However, with a less efficient ecosystem i.e. a smaller N , the Archean steady-state O_2 value decreases and the oxidation window is shortened due to a faster GOE transition (see supplementary materials). In this model the most unfavorable case is $N = 10^{-3}\zeta$ which corresponds to the minimum value of N leading to the appearance of the GOE in the simulation and therefore to coherent solutions. This critical

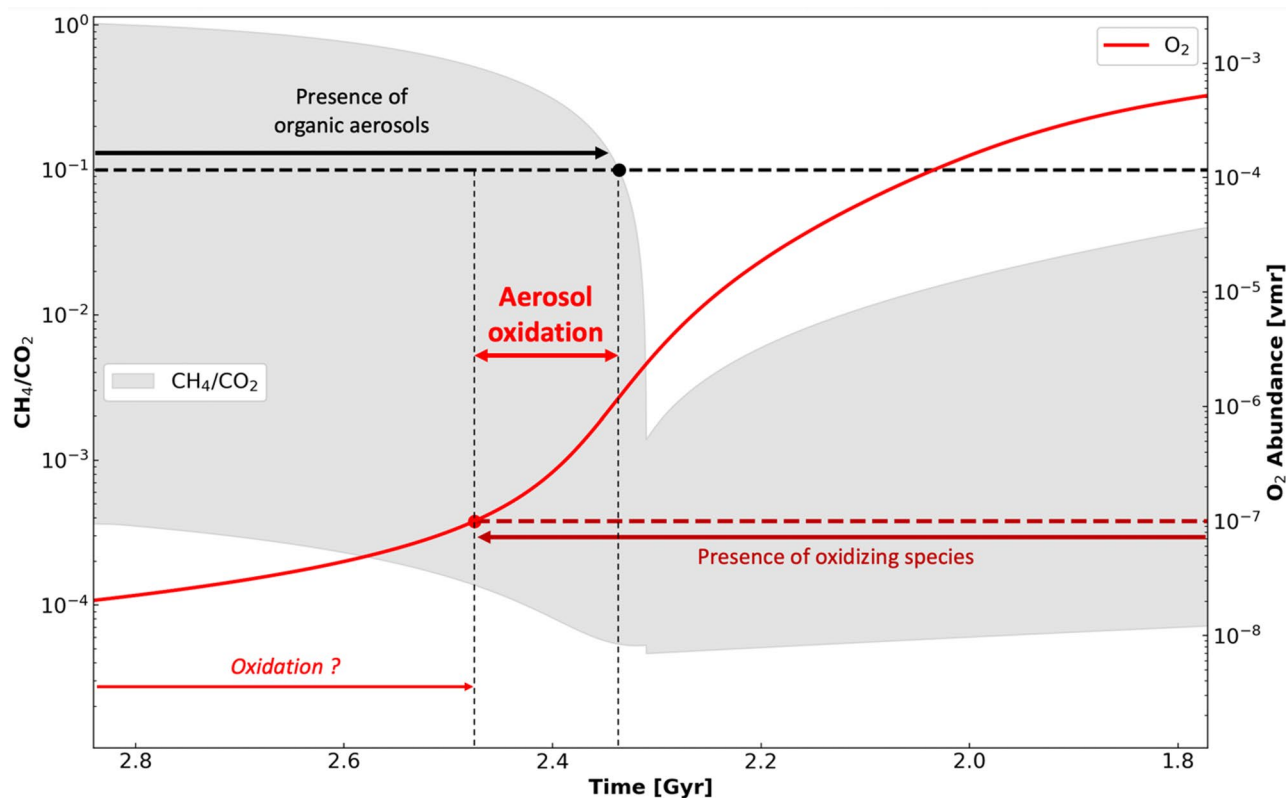


Fig. 3. On the left axis is shown the uncertainties of the ratio CH_4/CO_2 with times. The black dashed line indicates the condition used for aerosol existence $\text{CH}_4/\text{CO}_2 > 0.1$. On the right axis the O_2 volume mixing ratio (vmr) is plotted in red. The red dashed line reminds the O_2 exposure value for the aerosols performed in this work and the criteria used for oxidation. The time line here is voluntarily restricted between 1.8 and 2.8 Gyrs to focus on the GOE. In the Early Archean before 2.8 Gyrs, the O_2 vmr and the CH_4/CO_2 do not change significantly.

value of N gives an estimation of the shortest possible oxidation window with this approach. In this latter case, the oxidation occurs between 2.34 and 2.28 Gyrs and lasts 60 Myrs.

To conclude on the aerosol oxidation timescale, in all the scenarios described above, aerosol oxidation processes could have persisted during significant timescales between 60 and 100 Myrs. Depending on the net primary productivity by oxygenic photosynthesis, N , the oxidation window could have been more precisely in the ranges 2.47–2.34 or 2.34–2.28 Gyrs with a potential extension in the Archean for the former case. The typical timescales highlighted here are therefore longer enough to envisage global impacts for the Early-Earth and its ecosystem.

Discussion

Impact of oxidation processes on early-earth ecosystems

The atmospheric oxidation of the organic haze, as previously shown in this work, would benefit the biosphere by providing directly or indirectly nutrients. Here we want to give examples of metabolisms susceptible to take advantage of these oxidized organic resources and consider the specific role of the main molecules observed.

The actual knowledge of the Neoproterozoic ecosystem is limited. However geological evidences as well as environmental constraints on available resources have further improved our representation of this system. Isotopic anomalies, recorded in Archean rocks on carbon¹² sulfur³⁹ and iron^{40,41} have been attributed to biological fractionation caused by methanogens, sulfur, and iron-metabolising microorganisms, respectively. The discovery of cyanobacteria microfossils⁴² coupled with phylogenetic approach⁴³ also suggests the existence of oxygenic photosynthesis since the Paleoproterozoic.

In this already diversified Archean ecosystem as we currently understand it, several heterotroph organisms are known to use oxidized organic matter. For instance, Methanogens reduce carbon to produce methane and consequently need an input of a higher oxidation state carbon. If CO_2 is a common oxidized resource for methanogens, other carbon substrates such as methyl organics, acetate, or formate^{43,44} are also used in the methanogenesis. Sulfur-reducing⁴⁵ and iron-reducing bacteria⁴⁶ are other examples of anaerobic organisms working with oxidized organic matter. In these metabolisms, sulfur and iron are further reduced by the oxidation of carbon into CO_2 . For both sulfur and iron bacteria types, oxidized organic substrates can take many diversified forms^{47,48}. These non-exhaustive examples highlight the importance of oxidized organics in general and carboxylic acid derivatives in particular. This intermediary redox state indeed allows to be implied in very

different metabolisms performing carbon oxidation as well as carbon reduction. The detection of carboxylic acids in our experiment confirms the possibility for aerosol oxidation mechanisms to be a global source of relevant organic nutrients in addition to photosynthesis.

Moreover, among the molecules previously identified, oxalic acid and urea have a distinct influence on the biosphere due to their inherent chemical properties. A significative indirect influence of oxalate for Early-Earth ecosystems is its ability to solubilize the iron(II) contained in rocks thanks to the formation of a divalent complex⁴⁹. This strong affinity of oxalate for iron could have increased the availability of Fe²⁺ nutrients for iron oxidizing phototrophs present in the Early-Earth oceans. Urea on the other side could have been a privileged nutrient for cyanobacteria. Modern cyanobacteria easily fix nitrogen resources and more particularly urea thanks to urease enzyme which hydrolyses urea into ammonia and carbon dioxide⁵⁰. Urease-encoding genes are found in the cyanobacteria genome⁵¹ but the question of nitrogen fixation in early-lineage of evolution remains an issue to address⁵². Finally, another important indirect impact of such oxidized organic matter relies on its reactivity notably on mineral surfaces. Evaporation/precipitation cycles on mineral induces a particularly efficient chemistry susceptible to transform the previous molecules into a second generation of organics having a different impact⁵³. The question of evolution of organic matter at the surface is therefore central to better assess its potential impacts at planetary scale.

In conclusion, all these elements point out the nutritive role of oxidized organic matter induced by aerosol oxidation processes for early ecosystems. Such oxygenated molecules constitute a new source of carbon for the heterotroph species whose contribution should be considered in the global carbon cycle. This input of oxidized organic matter from aerosols could have been significant for the heterotroph organisms i.e. comparable to the flux of C produced by primary oxygenic photosynthesis. Experiments²³ and models⁵⁴ estimate a flux of organic matter from haze at the surface of the Early-Earth between 10¹³ and 10¹⁵ g of C.yr⁻¹, which corresponds respectively to 1/1000 and 1/10 of primary carbon production by modern marine ecosystem. Such values are within the order of magnitude of the primary production of the Early-Earth ecosystem which is described in the literature as less efficient⁵⁵ compared to nowadays. Moreover, such mechanisms could have provided different types of organic substrates than photosynthesis thus generating a diversified pool of available nutrients for the ecosystem. This wide diversity of molecules from different sources and processes have probably been an important vector of biodiversity for the primitive ecosystem. The understanding of the occurrence and the dynamic of the GOE also lies in a more detailed description of the Archaean ecosystem and its biodiversity.

Methods

Aerosol synthesis

Tholins were produced from a N₂/CH₄ mixture (96.5:4.5) in an AC cold Plasma setup called PAMPRE⁵⁶ at a pressure of 1mbar, a flowrate of 55 sccm (Standard Cubic Centimeter per Minutes) and a power of 30 W. Such experiment aims to simulate the upper layer of Early-Earth atmosphere, in which the incoming rays are sufficiently energetic to trigger a complex chemistry leading to the formation of solid particles.

Then the aerosols were collected and stored for ten days under a controlled atmosphere (0.1 ppm O₂ and 1ppm H₂O) in a glovebox (Jacomex BS 531). This proportion in O₂ represents an experimental limit that cannot be exceeded due to the capacity of the glovebox and the residual vacuum in the plasma chamber which is under primary pumping (10⁻³ mbar). Such exposure aims to study chemical evolution of reduced aerosols in the atmosphere and/or at the surface after their sedimentation. Oxidizing species such as OH radicals are indeed susceptible to react with reduced organic hazes.

Analytical protocol

Prior to injection into the GC-MS, the collected hazes were derivatized with a solution of MTBSTFA: DMF (acronyms for DiMethylFormamide and *N-Tert-Butyldimethylsilyl-N-méthylTriFluoroAcétamide*) (4:1 in volume) containing naphthalene-d₈ as an internal standard. This derivatization protocol was used here to enhance the detection of the polar oxidized molecules by replacing their labile hydrogens into a *Tert-Butyldimethylsilyl* group (*t*-BDMS), making them more amenable to GC-MS. The reaction was performed at 75 °C during 15 min with a concentration of 3 mg of sample for 40 μL. Three replicates of this derivatized solution were prepared as well as a blank reference sample composed of an empty vial stored in the same conditions and duration as the aerosols. A derivatization was also performed in this vial and constitute the blank reference sample plotted in Fig. 1. The DMF (Purity > 99%) and MTBSTFA reagents (Purity > 99%) as well as the naphthalene-d₈ standard (99%D, Purity > 98%) were purchased at sigma-Aldrich.

Finally, 1 μL of the derivatized solution was injected in the GC-MS for analysis (Thermo scientific Trace 1300 GC coupled with a Thermo scientific ISQ Ion Single Quadrupole mass spectrometer) on a RT-X20 capillary column. The temperature of the GC column was initially 60 °C followed by two ramps of 5 °C.min⁻¹ up to 150 °C and 10 °C.min⁻¹ up to 300 °C, and finally held at this temperature for 5 min. The split of Helium gas (Air liquide, purity > 99.999%) was 20 ml.min⁻¹. The mass spectrometry measurements were performed using an electronic impact ionization of 70 eV over a range of 40–600 mass units. The temperature of the line transfer and the source were both set at 300 °C.

The retention time validation of the different compounds has been performed on the same instrument using the same analytical method. The chemical standards urea, glycine, oxalic acid, ameline, 5-azacytosine and hydroxylamine used for this measurements were also purchased at Sigma-Aldrich, except ameline (Fischer Scientific).

O₂ variation model

The temporal evolution of O₂ vmr is calculated using the following system of coupled differential equations involving the functions $M(t)$ and $O(t)$ which represent respectively the absolute quantities of CH₄ and O₂

in mol. Ω_{O_2} , r , and Ψ_{O_2} are functions of $O(t)$, their parametrization is described more precisely in the following study³⁸. $s = 2.03 \times 10^{-5} \text{ yr}^{-1}$ is a fixed parameter for the hydrogen loss, whereas N represent the annual production of oxygen by marine photosynthesis. For the simulation Fig. 3, we assume a marine photosynthesis productivity $\dot{N} = 3.5 \times 10^{14} \text{ mol O}_2 \cdot \text{yr}^{-1}$ ten times inferior to modern marine ecosystem.

$$\left\{ \begin{array}{l} \frac{dM}{dt} = \frac{1}{2} \Omega_{O_2} (N + r) - sM - \frac{1}{2} \Psi_{O_2} M^{0.7} \quad (1) \\ \frac{d\Omega}{dt} = N \Omega_{O_2} - (1 - \Omega_{O_2})r - sM - \Psi_{O_2} M^{0.7} \quad (2) \end{array} \right.$$

Data availability

GC-MS data used and/or analysed during the current study available from the corresponding author on reasonable request.

Received: 1 April 2025; Accepted: 24 July 2025

Published online: 11 August 2025

References

- Farquhar, J., Bao, H. & Thiemens, M. Atmospheric influence of earth's earliest sulfur cycle. *Science* **289**, 756–758 (2000).
- Farquhar, J. et al. Isotopic evidence for mesoarchaeon anoxia and changing atmospheric sulphur chemistry. *Nature* **449**, 706–709 (2007).
- Farquhar, J., Savarino, J., Airieau, S. & Thiemens, M. H. Observation of wavelength-sensitive mass-independent sulfur isotope effects during SO₂ photolysis: implications for the early atmosphere. *J. Geophys. Res. Planet.* **106**, 32829–32839 (2001).
- Catling, D. C. & Zahnle, K. J. The archean atmosphere. *Sci. Adv.* **6**, eaax1420 (2020).
- Pavlov, A. A. & Kasting, J. F. Mass-independent fractionation of sulfur isotopes in archean sediments: strong evidence for an anoxic archean atmosphere. *Astrobiology* **2**, 27–41 (2002).
- Zahnle, K. J., Claire, M. W. & Catling, D. C. The loss of mass-independent fractionation in sulfur due to a paleoproterozoic collapse of atmospheric methane. *Geobiology* **4**, 271–283 (2006).
- Sheldon, N. Precambrian paleosols and atmospheric CO₂ levels. *Precambrian Res.* **147**, 148–155 (2006).
- Driese, S. G. et al. Neoproterozoic paleoweathering of tonalite and metabasalt: implications for reconstructions of 2.69 Ga early terrestrial ecosystems and paleoatmospheric chemistry. *Precambrian Res.* **189**, 1–17 (2011).
- Zahnle, K. J., Gacesa, M. & Catling, D. C. Strange messenger: A new history of hydrogen on earth, as told by Xenon. *Geochim. Cosmochim. Acta.* **244**, 56–85 (2019).
- Kurokawa, H., Foriel, J., Laneuville, M., Houser, C. & Usui, T. Subduction and atmospheric escape of earth's seawater constrained by hydrogen isotopes. *Earth Planet. Sci. Lett.* **497**, 149–160 (2018).
- Stueeken, E. E. & Buick, R. Environmental control on microbial diversification and methane production in the mesoarchean. <https://doi.org/10.1016/j.precamres.2017.11.003> (2018).
- Ueno, Y., Yamada, K., Yoshida, N., Maruyama, S. & Isozaki, Y. Evidence from fluid inclusions for microbial methanogenesis in the early Archean era. *Nature* **440**, 516–519 (2006).
- KHARECHA, P., Kasting, J. & Siefert, J. A coupled atmosphere–ecosystem model of the early archean Earth. *Geobiology* **3**, 53–76 (2005).
- Ozaki, K., Tajika, E., Hong, P. K., Nakagawa, Y. & Reinhard, C. T. Effects of primitive photosynthesis on earth's early climate system. *Nat. Geosci.* **11**, 55–59 (2018).
- Israël, G. et al. Complex organic matter in titan's atmospheric aerosols from in situ pyrolysis and analysis. *Nature* **438**, 796–799 (2005).
- Arney, G. et al. The pale orange dot: the spectrum and habitability of hazy archean Earth. *Astrobiology* **16**, 873–899 (2016).
- Haqq-Misra, J. D., Domagal-Goldman, S. D., Kasting, P. J. & Kasting, J. F. A revised, hazy methane greenhouse for the archean Earth. *Astrobiology* **8**, 1127–1137 (2008).
- Sagan, C. & Chyba, C. The early faint sun paradox: organic shielding of ultraviolet-labile greenhouse gases. *Science* **276**, 1217–1221 (1997).
- Zerkle, A. L., Claire, M. W., Domagal-Goldman, S. D., Farquhar, J. & Poulton, S. W. A bistable organic-rich atmosphere on the Neoproterozoic Earth. *Nat. Geosci.* **5**, 359–363 (2012).
- Izon, G. et al. Multiple oscillations in Neoproterozoic atmospheric chemistry. *Earth Planet. Sci. Lett.* **431**, 264–273 (2015).
- Thomazo, C., Nisbet, E., Grassineau, N., Peters, M. & Strauss, H. Multiple sulfur and carbon isotope composition of sediments from the Belingwe greenstone belt (Zimbabwe): A biogenic methane regulation on mass independent fractionation of sulfur during the neoproterozoic? *Geochim. Cosmochim. Acta.* **121**, 120–138 (2013).
- Flannery, D. et al. Spatially-resolved isotopic study of carbon trapped in ~3.43 Ga Strelley pool formation stromatolites. *Geochim. Cosmochim. Acta* **223**, (2017).
- Trainer, M. G. et al. Organic haze on Titan and the early Earth. *Proc. Natl. Acad. Sci. U. S. A.* **103**, 18035–18042 (2006).
- Fleury, B. et al. Influence of CO on Titan atmospheric reactivity. *Icarus* **238**, 221–229 (2014).
- Atkinson, R. & Arey, J. Atmospheric degradation of volatile organic compounds. *Chem. Rev.* **103**, 4605–4638 (2003).
- Rudich, Y., Donahue, N. M. & Mentel, T. F. Aging of organic aerosol: bridging the gap between laboratory and field studies. *Annu. Rev. Phys. Chem.* **58**, 321–352 (2007).
- Sprengnether, M., Demerjian, K. L., Donahue, N. M. & Anderson, J. G. Product analysis of the OH oxidation of isoprene and 1,3-butadiene in the presence of NO. *J. Geophys. Res. Atmos.* **107**, ACH 8-1–ACH 8-13 (2002).
- Volkamer, R. et al. OH-initiated oxidation of benzene. *Phys. Chem. Chem. Phys.* **4**, 1598–1610 (2002).
- Brassé, C., Buch, A., Coll & Raulin, F. Low-Temperature alkaline pH hydrolysis of Oxygen-Free Titan tholins: carbonates' impact. *Astrobiology* **17**, 8–26 (2017).
- Neish, C. D., Somogyi, Á. & Smith, M. A. Titan's primordial soup: formation of amino acids via Low-Temperature hydrolysis of Tholins. *Astrobiology* **10**, 337–347 (2010).
- Khare, B. N. et al. Amino acids derived from Titan Tholins. *Icarus* **68**, 176–184 (1986).
- Derenne, S. et al. New insights into the structure and chemistry of titan's Tholins via 13 C and 15 N solid state nuclear magnetic resonance spectroscopy. *Icarus* **221**, 844–853 (2012).
- Gautier, T. et al. Development of HPLC-Orbitrap method for identification of N-bearing molecules in complex organic material relevant to planetary environments. *Icarus* **275**, 259–266 (2016).
- Morisson, M., Szopa, C., Carrasco, N., Buch, A. & Gautier, T. Titan's organic aerosols: molecular composition and structure of laboratory analogues inferred from pyrolysis gas chromatography mass spectrometry analysis. *Icarus* **277**, 442–454 (2016).
- Quirico, E. et al. New experimental constraints on the composition and structure of Tholins. *Icarus* **198**, 218–231 (2008).
- Maillard, J. et al. Humid evolution of haze in the atmosphere of Super-Earths in the habitable zone. *Astrobiology* **23**, 723–732 (2023).

37. Poch, O., Coll, P., Buch, A., Ramírez, S. I. & Raulin, F. Production yields of organics of Astrobiological interest from H₂O–NH₃ hydrolysis of titan's Tholins. *Planet. Space Sci.* **61**, 114–123 (2012).
38. Jaziri, A. Y., Charnay, B., Selsis, F., Leconte, J. & Lefèvre, F. Dynamics of the great oxidation event from a 3D photochemical–climate model. *Clim. Past.* **18**, 2421–2447 (2022).
39. Velivetskaya, T. A., Ignatiev, A. V., Vysotskiy, S. V. & Aseeva, A. V. Ratios of sulfur isotopes (32S, 33S, 34S, and 36S) in archean rocks of karelia: evidence of microbial life and the anoxic atmosphere. *Russ Geol. Geophys.* **65**, 689–698 (2024).
40. Archer, C. & Vance, D. Coupled Fe and S isotope evidence for archean microbial Fe(III) and sulfate reduction. *Geology* **34**, 153–156 (2006).
41. Craddock, P. R. & Dauphas, N. Iron and carbon isotope evidence for microbial iron respiration throughout the archean. *Earth Planet. Sci. Lett.* **303**, 121–132 (2011).
42. Schopf, J. W. The fossil record of cyanobacteria. in *Ecology of Cyanobacteria II: their Diversity in Space and time* (ed Whitton, B. A.) 15–36 (Springer Netherlands, Dordrecht, doi:https://doi.org/10.1007/978-94-007-3855-3_2. (2012).
43. de Bueno, C. P., Wu, D. & Tringe, S. G. Methyl-Based methanogenesis: an ecological and genomic review. *Microbiol. Mol. Biol. Rev. MMBR.* **87**, e00024–e00022 (2013).
44. Blaut, M. Metabolism of methanogens. *Antonie Van Leeuwenhoek.* **66**, 187–208 (1994).
45. Schauder, R. & Kröger, A. Bacterial sulphur respiration. *Arch. Microbiol.* **159**, 491–497 (1993).
46. Ebrahiminezhad, A., Manafi, Z., Berenjian, A., Kianpour, S. & Ghasemi, Y. Iron-Reducing bacteria and iron nanostructures. *J. Adv. Med. Sci. Appl. Technol.* **3**, 9 (2017).
47. Bonch-Osmolovskaya, E. A., Sokolova, T. G., Kostrikina, N. A. & Zavarzin, G. A. *Desulfurella acetivorans* gen. Nov. And sp. Nov. —a new thermophilic sulfur-reducing Eubacterium. *Arch. Microbiol.* **153**, 151–155 (1990).
48. Straub, K. L. & Buchholz-Cleven, B. E. *Geobacter Bremensis* sp. Nov. And *geobacter pelophilus* sp. Nov., two dissimilatory ferric-iron-reducing bacteria. *Int. J. Syst. Evol. Microbiol.* **51**, 1805–1808 (2001).
49. Veglió, F., Passariello, B., Barbaro, M., Plescia, P. & Marabini, A. M. Drum leaching tests in iron removal from quartz using oxalic and sulphuric acids. *Int. J. Min. Process.* **54**, 183–200 (1998).
50. Veaudor, T., Cassier-Chauvat, C. & Chauvat, F. Genomics of Urea transport and catabolism in cyanobacteria: biotechnological implications. *Front. Microbiol.* **10**, 2052 (2019).
51. Solomon, C., Collier, J., Berg, G. & Glibert, P. Role of Urea in microbial metabolism in aquatic systems: a biochemical and molecular review. *Aquat. Microb. Ecol.* **59**, 67–88 (2010).
52. Grettenberger, C. L. et al. A phylogenetically novel Cyanobacterium most closely related to *Gloeobacter*. *ISME J.* **14**, 2142–2152 (2020).
53. Lahav, N., White, D. & Chang, S. Peptide formation in the prebiotic era: thermal condensation of Glycine in fluctuating clay environments. *Science* **201**, 67–69 (1978).
54. Wolf, E. T. & Toon, O. B. Fractal organic hazes provided an ultraviolet shield for early Earth. *Science* **328**, 1266–1268 (2010).
55. Canfield, D. E., Rosing, M. T. & Bjerrum, C. Early anaerobic metabolisms. *Philos. Trans. R Soc. B Biol. Sci.* **361**, 1819–1836 (2006).
56. Szopa, C., Cernogora, G., Boufendi, L., Correia, J. J. & Coll, P. PAMPRE: A dusty plasma experiment for titan's Tholins production and study. *Planet. Space Sci.* **54**, 394–404 (2006).

Acknowledgements

We would like to thank Pr Charles Cockell for his advice and fruitful discussions.

Author contributions

L.M wrote the main manuscript. M.M, N.C, V.M, A.J reviewed the main manuscript. A.J provides the code of photochemical models monitoring the evolution of o₂ during the Archean and the Great-Oxidation-Event. V.M, T.G, L.V, A.A were implied in the experiments of the article.

Declarations

Competing interests

The authors declare no competing interests.

Additional information

Supplementary Information The online version contains supplementary material available at <https://doi.org/10.1038/s41598-025-13441-1>.

Correspondence and requests for materials should be addressed to L.M.

Reprints and permissions information is available at www.nature.com/reprints.

Publisher's note Springer Nature remains neutral with regard to jurisdictional claims in published maps and institutional affiliations.

Open Access This article is licensed under a Creative Commons Attribution 4.0 International License, which permits use, sharing, adaptation, distribution and reproduction in any medium or format, as long as you give appropriate credit to the original author(s) and the source, provide a link to the Creative Commons licence, and indicate if changes were made. The images or other third party material in this article are included in the article's Creative Commons licence, unless indicated otherwise in a credit line to the material. If material is not included in the article's Creative Commons licence and your intended use is not permitted by statutory regulation or exceeds the permitted use, you will need to obtain permission directly from the copyright holder. To view a copy of this licence, visit <http://creativecommons.org/licenses/by/4.0/>.

© The Author(s) 2025